

1 Concentrations and stable carbon isotope compositions of oxalic
2 acid and related SOA in Beijing before, during and after the
3 2014 APEC
4
5
6
7
8
9

10 Jiayuan Wang^{1,3}, Gehui Wang^{1,2,3,4,*}, Jian Gao^{5,6,*}, Han Wang^{5,6}, Yanqin Ren^{1,3},
11 Jianjun Li¹, Bianhong Zhou¹, Can Wu^{1,3}, Lu Zhang^{1,3}, Shulan Wang^{5,6}, Fafe Chai^{5,6}
12
13
14
15
16
17
18
19
20
21

22 ¹State Key Laboratory of Loess and Quaternary Geology, Key Lab of Aerosol Chemistry and
23 Physics, Institute of Earth Environment, Chinese Academy of Sciences, Xi'an 710061, China

24 ²School of Human Settlements and Civil Engineering, Xi'an Jiaotong University, Xi'an 710079,
25 China

26 ³University of Chinese Academy of Sciences, Beijing 100049, China

27 ⁴Center for Excellence in Regional Atmospheric Environment, Institute of Urban Environment,
28 Chinese Academy of Sciences, Xiamen 361021, China

29 ⁵State Key Laboratory of Environmental Criteria and Risk Assessment, Chinese Research
30 Academy of Environmental Sciences, Beijing 100084, China

31 ⁶Collaborative Innovation Center of Atmospheric Environment and Equipment Technology,
32 Nanjing 210000, China
33
34
35
36

37 *Correspondence to:* Gehui Wang (wanggh@ieecas.cn) and Jian Gao (gaojian@craes.org.cn)
38
39
40
41

42 **Abstract:** To ensure the good air quality for the 2014 APEC, stringent emission controls were
43 implemented in Beijing and its surrounding regions, leading to a significant reduction in PM_{2.5}
44 loadings. To investigate the impact of the emission controls on aerosol chemistry, high-volume
45 PM_{2.5} samples were collected in Beijing from 8th October to 24th November, 2014 and
46 determined for secondary inorganic ions (SIA, i.e., SO₄²⁻, NO₃⁻ and NH₄⁺), dicarboxylic acids,
47 keto-carboxylic acid and α -dicarbonyls, as well as stable carbon isotope composition of oxalic
48 acid (C₂). Our results showed that SIA, C₂ and related SOA in PM_{2.5} during-APEC were 2–4
49 times lower than those before-APEC, which is firstly ascribed to the strict emission control
50 measures and secondly attributed to the relatively colder and drier conditions during the event
51 that are unfavorable for secondary aerosol production.

52 C₂ in the polluted air masses, which mostly occurred before-APEC, are abundant and
53 enriched in ¹³C. On the contrary, C₂ in the clean air masses, which mostly occurred during-APEC,
54 is much less abundant but still enriched in ¹³C. In the mixed type of clean and polluted air
55 masses, which mostly occurred after-APEC, C₂ is lower than that before-APEC but higher than
56 that during-APEC and enriched in lighter ¹²C. A comparison on chemical composition of fine
57 particles and $\delta^{13}\text{C}$ values of C₂ in two events that are characterized by high loadings of PM_{2.5}
58 further showed that after-APEC SIA and the total detected organic compounds (TDOC) are
59 much less abundant and fine aerosols are enriched with primary organics and relatively fresh,
60 compared with those before-APEC.

61

62 **Key words:** Secondary organic aerosols; Emission controls; Sources and formation mechanisms;
63 Aqueous-phase oxidation; Aerosol acidity and water content.

64 **1. Introduction**

65 Atmospheric aerosols profoundly impact the global climate directly by scattering and
66 absorbing solar radiation and indirectly by affecting cloud formation and distribution via acting
67 as cloud condensation nuclei (CCN) and ice nuclei (IN). Moreover, atmospheric aerosols exert
68 negative effects on human health because of their toxicity. Due to fast urbanization and
69 industrialization, high level of atmospheric fine particle (PM_{2.5}) pollution has been a persistent
70 problem in many cities of China since the nineties of last century (van Donkelaar et al., 2010).
71 As the capital of China and one of the largest megacities in the world, Beijing has suffered from
72 frequent severe haze pollution especially in winter, affecting more than 21 million people by the
73 end of 2014 (Beijing Municipal Bureau of Statistics, 2015) and causing billions of economic
74 losses (Mu and Zhang, 2013). To improve the air quality Beijing government has put many efforts
75 to reduce the pollutant emissions (i.e., SO₂, NO_x, dust, and volatile organic compounds (VOCs))
76 from a variety of sources.

77 The 2014 Asia-Pacific Economic Cooperation (APEC) summit was hosted in Beijing from
78 the 5th to 11th November. To ensure good air quality for the summit, a joint strict emission control
79 program was conducted from 3rd November 2014 in Beijing and its neighboring provinces
80 including Inner Mongolia, Shanxi, Hebei and Shandong provinces. During this period thousands
81 of factories and power plants with high emissions were shut down and/or halted, all the
82 construction activities were stopped and the numbers of on-road vehicles were reduced. These
83 strict emission controls resulted in the air quality of Beijing during the APEC period being
84 significantly improved, leading to a decrease in PM_{2.5} concentration by 59.2% and an increase in
85 visibility by 70.2% in Beijing during the summit compared with those before the APEC (Tang et

86 al., 2015; Wang et al., 2015b) and a term of “APEC-Blue” being created to refer to the good air
87 quality. Such strong artificial intervening not only reduced PM_{2.5} and its precursors’ loadings in
88 Beijing and its surrounding areas but also affected the composition and formation mechanisms of
89 the fine particles (Sun et al., 2016).

90 A number of field measurements have showed that particle compositions in Beijing during
91 wintertime haze periods are dominated by secondary aerosols (Guo et al., 2014; Huang et al.,
92 2014; Xu et al., 2015). Rapid accumulation of particle mass in Beijing during haze formation
93 process is often accompanied by continuous particle size growth (Guo et al, 2014; Zhang et al.,
94 2015), which is in part due to the coating of secondary organic aerosols (SOA) on pre-existing
95 particles (Li et al., 2010). Several studies have found that SOA production during the 2014
96 Beijing APEC periods significantly reduced and ascribed this reduction to the efficient regional
97 emission control (Sun et al., 2016; Xu et al, 2015). However, up to now information of the SOA
98 decrease on a molecular level has not been reported.

99 Dicarboxylic acids are the major class of SOA species in the atmosphere and ubiquitously
100 found from the ground surface to the free troposphere (Fu et al., 2008; Myriokefalitakis et al.,
101 2011; Sorooshian et al., 2007; Sullivan et al., 2007). Previous studies have suggested that organic
102 acids including dicarboxylic acids could take part in atmospheric particle nucleation (Zhang et
103 al., 2004; Zhao et al., 2009) and growth processes (Zhang et al., 2012). Furthermore, organic
104 acids may play a central role in aging of black carbon particles (Xue et al., 2009; Ma et al., 2013),
105 enhancing their roles in air pollution accumulation and direct radiative forcing (Peng et al., 2016).
106 In the current work we measured molecular distributions of dicarboxylic acids, keto-carboxylic
107 acids and α -dicarbonyls and stable carbon isotope composition of oxalic acid in PM_{2.5} aerosols

108 collected in Beijing before, during and after the APEC event in order to explore the impact of the
109 APEC emission control on SOA in Beijing. We first investigated the changes in concentration
110 and composition of dicarboxylic acids and related compounds during the three periods, then
111 recognized the difference in stable carbon isotope composition of oxalic acid in different air
112 masses in Beijing during the APEC campaign. Finally we compared the differences in chemical
113 compositions of PM_{2.5} during two heaviest pollution episodes.

114 **2. Experimental section**

115 **2.1 Sample collection**

116 PM_{2.5} samples were collected by using a high-volume sampler (TISCH, USA) from 8th
117 October to 24th November 2014 on the rooftop of a three-storey building located on the campus
118 of China Research Academy of Environmental Sciences, which is situated in the north part of
119 Beijing and close to the 5th-ring road. All the PM_{2.5} samples were collected onto pre-baked (450
120 °C for 8 h) quartz fiber filters (Whatman 41, USA). The duration of each sample collection is 23
121 hr from 08:00 am of the previous day to 07:00 am of the next day. Field blanks were also
122 collected before and after the campaign by mounting a pre-baked filter onto the sampler for 15
123 min without pumping air. After collection, all the filter samplers were individually sealed in
124 aluminum foil bags and stored in a freezer (-18 °C) prior to analysis. Daily values of SO₂, NO_x
125 and meteorological parameters were cited from the website of Beijing Environmental Protection
126 Agency.

127 **2.2 Sample analysis**

128 **2.2.1 Elemental carbon (EC), organic carbon (OC), water-soluble organic (WSOC),**
129 **inorganic ions, aerosol liquid water content (ALWC) and aerosol acidity**

130 Detailed methods for the analysis of EC, OC, WSOC and inorganic ions in aerosols were
131 reported elsewhere (Wang et al 2010). Briefly, EC and OC in the PM_{2.5} samples were determined
132 by using DRI Model 2001 Carbon analyzer following the Interagency Monitoring of Protected
133 Visual Environments (IMPROVE) thermal/optical reflectance (TOR) protocol (Chow et al.,
134 2007). WSOC and inorganic ions in the samples were extracted with Milli-Q pure water and
135 measured by using Shimadzu TOC-L CPH analyzer and Dionex-600 ion chromatography,
136 respectively (Wang et al 2010). In the current work, aerosol liquid water content (ALWC) and
137 acidity (i.e., liquid H⁺ concentrations, [H⁺]) of the samples were calculated by using
138 ISORROPIA-II model, which treated the Na⁺-NH₄⁺-K⁺-Ca²⁺-Mg²⁺-Cl⁻-NO₃⁻-SO₄²⁻ system
139 and was performed in a “metastable” mode (Hennigan et al, 2015; Weber et al., 2016).

140 **2.2.2 Dicarboxylic acids, keto-carboxylic acids and α -dicarbonyls**

141 The method of analyzing PM_{2.5} samples for dicarboxylic acids, ketocarboxylic acids and
142 α -dicarbonyl has been reported elsewhere (Wang et al., 2002, 2012; Meng et al., 2014; Cheng et
143 al., 2015). Briefly, one eighth of the filter was extracted with Milli-Q water, concentrated to near
144 dryness, and reacted with 14% BF₃/butanol at 100 °C for 1 h to convert aldehyde group into
145 dibutoxy acetal and carboxyl group into butyl ester. Target compounds in the derivatized samples
146 were identified by GC/MS and quantified by GC-FID (Agilent GC7890A).

147 **2.3. Stable carbon isotope composition of oxalic acid (C₂)**

148 Stable carbon isotope composition ($\delta^{13}\text{C}$) of C₂ was measured using the method developed
149 by Kawamura and Watanabe (2004). Briefly, $\delta^{13}\text{C}$ values of the derivatized samples above were
150 determined by gas chromatography-isotope ratio-mass spectrometry (GC-IR-MS) (Thermo
151 Fisher, Delta V Advantage). The $\delta^{13}\text{C}$ value of C₂ was then calculated from an isotopic mass

152 balance equation based on the measured $\delta^{13}\text{C}$ of the derivatizations and the derivatizing reagent
153 (1-butanol) (Kawamura and Watanabe, 2004). Each sample was measured for three times to
154 ensure the difference of the $\delta^{13}\text{C}$ values less than 0.2‰, and the isotope data reported here is the
155 averaged value of the triplicate measurements.

156 **3. Results and discussion**

157 **3.1 Variations in meteorological conditions, gaseous pollutants and major components of** 158 **PM_{2.5} during the Beijing 2014 APEC campaign**

159 Based on the emission control implementation for the APEC, we divided the whole study
160 period into three phases: before-APEC (08/10 to 02/11), during-APEC (03/11 to 12/11) and
161 after-APEC (13/11 to 24/11). Temporal variations in meteorological parameters and
162 concentrations of gaseous pollutants and major components of PM_{2.5} during the three phases are
163 shown in Fig. 1 and summarized in Table 1.

164 Temperature during the sampling campaign showed a continuous decreasing trend with
165 averages of 13 ± 2.6 °C, 7.0 ± 1.7 °C and 4.3 ± 1.3 °C before-, during- and after-APEC periods,
166 respectively, while relative humidity (RH) did not show a clear trend with mean values of $62 \pm$
167 19% , $47 \pm 14\%$ and $51 \pm 16\%$ during the three periods (Fig.1a and Table 1). SO₂ showed a
168 similar level before- and during-APEC periods (8.8 ± 4.6 $\mu\text{g m}^{-3}$ versus 7.6 ± 3.9 $\mu\text{g m}^{-3}$) (Table
169 1 and Fig.1b), but increased dramatically to 23 ± 8.8 $\mu\text{g m}^{-3}$ after-APEC due to domestic coal
170 burning for house heating. NO₂ concentration (45 ± 18 $\mu\text{g m}^{-3}$) during the APEC reduced by
171 about 30% compared to that in the before- and after-APEC phases (71 ± 27 $\mu\text{g m}^{-3}$ versus $78 \pm$
172 29 $\mu\text{g m}^{-3}$) (Table 1), mainly because of the reduction of the on-road vehicle numbers, as well as
173 the reduced productivities of power plant and industry. O₃ displayed a decreasing trend similar to

174 that of temperature (Fig. 1c). PM_{2.5} pollution episodes in Beijing showed a periodic cycle of 4–5
175 days, which is caused by the local weather cycles. Secondary inorganic ions (SIA, i.e., SO₄²⁻,
176 NO₃⁻ and NH₄⁺) are major components of PM_{2.5} and present a temporal variation pattern similar
177 to that of the fine particles (Fig. 1d). In the current work mass ratio of NO₃⁻/SO₄²⁻ in PM_{2.5}
178 during the whole study time is 1.8 ± 1.9 (Table 1), which is in agreement with the ratio (1.6–2.4)
179 for PM₁ observed during the same time by using aerosol mass spectrometry (AMS) (Sun et al.,
180 2016). OC and EC of PM_{2.5} linearly correlated each other (R²=0.91) and varied periodically in a
181 cycle similar to SIA (Fig. 1e). OC/EC ratio during the whole sampling period is 3.3 ± 0.6 (range:
182 2.2–4.7) with no significant differences among the three APEC phases (Table 1), although the
183 source emissions could be largely different.

184 Figure 2 shows the differences in chemical composition of PM_{2.5} before-, during- and
185 after-APEC periods. PM_{2.5} is 98 ± 46 μg m⁻³ during-APEC, about 50% lower than that before-
186 and after-APEC (178 ± 122 μg m⁻³ versus 161 ± 100 μg m⁻³), respectively. Organic matter (OM)
187 is the most abundant component of the fine particles. Relative abundance of OM (OM, 1.6 times
188 of OC) (Xing et al., 2013) to PM_{2.5} continuously increases from 24% before-APEC to 30% and
189 39% during- and after-APEC, respectively, although the mass concentration (19 ± 7.6 μg m⁻³) of
190 OC during-APEC is the lowest compared to those before- and after-APEC (26 ± 16 μg m⁻³
191 versus 39 ± 23 μg m⁻³). Sulfate, nitrate and ammonium before-APEC are 15 ± 13, 28 ± 26 and
192 9.0 ± 8.0 μg m⁻³ (Table 1) and account for 8%, 16% and 5% of PM_{2.5}, respectively (Fig. 2). Their
193 concentrations decrease to 5.3 ± 2.8, 10 ± 8.1 and 3.1 ± 2.6 μg m⁻³ (Table 1) with the relative
194 contributions to PM_{2.5} down to 5%, 10% and 3% during-APEC, respectively. While after-APEC
195 their concentrations increased to 11 ± 10, 15 ± 13 and 6.9 ± 6.4 μg m⁻³ and accounted for 7%,

196 9% and 4% of $PM_{2.5}$. Such significant decreases in concentrations of OM and SIA during-APEC
197 demonstrate the efficiency of the emission controls. OC/EC ratio is almost constant during the
198 whole period, but WSOC/OC ratio decreased by 20% from 0.42 ± 0.13 before-APEC, $0.38 \pm$
199 0.16 during-APEC to 0.35 ± 0.17 after-APEC (Table 1). Since WSOC in fine aerosols consist
200 mainly of secondary organic aerosols (SOA) (Laskin et al., 2015), the decreasing ratio of
201 WSOC/OC probably indicates a reduced SOA production during the campaign.

202 **3.2 Oxalic acid and related SOA during the Beijing 2014 APEC campaign**

203 A homogeneous series of dicarboxylic acids (C_2 - C_{11}), keto-carboxylic acid and
204 α -dicarbonyls in the $PM_{2.5}$ samples were detected. As show in Table 2, total dicarboxylic acids
205 during the whole study period is $593 \pm 739 \text{ ng m}^{-3}$, which is lower than that observed during
206 Campaign of Air Quality Research in Beijing 2006 (CAREBeijing) (average 760 ng m^{-3}) and
207 2007 (average 1010 ng m^{-3}) (Ho et al, 2010, 2015) and the averaged wintertime concentration
208 reported by a previous research for 14 Chinese cities (904 ng m^{-3}) (Ho et al, 2007). Total
209 keto-carboxylic acid is $66 \pm 81 \text{ ng m}^{-3}$, while total dicarbonyls is $126 \pm 115 \text{ ng m}^{-3}$ (Table 2).
210 These values are higher than those during CAREBeijing 2006 and 2007 (Ho et al, 2010, 2015),
211 but close to the value observed for the 14 Chinese megacities (Ho et al, 2007). Being similar to
212 those previous observations, oxalic acid (C_2) is the most abundant diacid in the 2014 APEC
213 samples with an average of $334 \pm 461 \text{ ng m}^{-3}$ (range: 10–2127 ng m^{-3} , Table 2) during the whole
214 campaign, followed by methylglyoxal (mGly), succinin acid (C_4), terephthalic acid (tPh), and
215 glyoxal (Gly). These five species account for 43%, 10%, 9%, 6% and 6% of total detected
216 organic compounds (TDOC), respectively (Fig. 3).

217 As see in Fig. 4, TDOC in $PM_{2.5}$ are 1099 ± 1104 , 325 ± 220 and $487 \pm 387 \text{ ng m}^{-3}$ before-,

218 during- and after-APEC, respectively. In comparison with those before-APEC, TDOC
219 during-APEC decreased by 71%. Oxalic acid (C_2) is the leading species among the detected
220 organic compounds and accounted for 46%, 31% and 34% of TDOC during the three phases,
221 respectively (Fig. 4). C_2 is an end product of precursors that are photochemically oxidized in
222 aerosol aqueous phase via either oxidation of small compounds containing two carbon atoms or
223 decomposition of larger compounds containing three or more carbon atoms. Thus mass ratio of
224 C_2 to TDOC is indicative of aerosol aging (Wang et al., 2012; Ho et al., 2015). As shown in Fig.
225 4, the highest proportion of C_2 before- APEC suggests that organic aerosols during this period are
226 more oxidized, compared to those during- and after-APEC. Glyoxal (Gly) and methylglyoxal
227 (mGly) are the precursors of C_2 . Mass ratios of both compounds to TDOC are lowest
228 before-APEC (Fig. 4), further indicating an enhanced SOA production during this period.

229 **3.3 Formation mechanism of oxalic acid**

230 **3.3.1 Correlation of oxalic acid with temperature, relative humidity (RH), aerosol liquid** 231 **water content (ALWC) and acidity and sulfate**

232 A few studies have pointed out that aerosol aqueous phase oxidation is a major formation
233 pathway for oxalic acid (Yu et al., 2005; van Pinxteren, et al., 2014; Bikkina et al., 2015; Tilgner
234 et al, 2010). To explore the formation mechanism of oxalic acid, we calculated ALWC and
235 acidity (i.e., proton concentration, $[H^+]$) of $PM_{2.5}$ aerosols by using ISOROPPIA-II model
236 (Weber et al., 2016). As shown in Fig. 5, during the entire period C_2 showed a strong linear
237 correlation with sulfate ($R^2=0.70$ Fig. 5a), which is consistent with those observed in Xi'an
238 (Wang et al., 2012) and other Chinese cities (Yu et al, 2005). Previous studies on particle
239 morphology showed that sulfate particles internally mixes with SOA in Beijing especially on

240 humid haze days (Li et al., 2010, 2011), which probably indicates that they are formed via
241 similar aqueous phase pathways (Wang et al., 2016). In addition, a robust correlation was also
242 found for C₂ with RH (R²=0.64, Fig. 5b) and aerosol liquid water content (ALWC) (R²=0.61, Fig.
243 5c), indicating that humid conditions are favorable for the aqueous phase formation of C₂, which
244 is most likely due to an enhanced gas-to-aerosol aqueous phase partitioning of the precursors
245 (e.g., Gly and mGly) (Fu et al., 2008; Wang et al., 2015a).

246 NH₄⁺, NO₃⁻ and SO₄²⁻ are the dominant cation and anions of fine particles in Beijing,
247 respectively (Guo et al., 2014; Zhang et al., 2015) and the molar ratio of [NH₄⁺] to [NO₃⁻] +
248 [SO₄²⁻] in this study is 1.1. Thus it is plausible that SO₄²⁻ during the APEC campaign largely
249 existed as ammonium bisulfate, resulting in a strong linear correlation between [H⁺] and SO₄²⁻
250 with a molar slope of 1.03 (Fig. 5d) (Zhang et al., 2007). In addition, [H⁺] shows a significant
251 positive correlation with C₂ (R² = 0.84) (Fig. 5e), possibly due to the fact that acidic conditions
252 are favorable for the formation of C₂ precursors. For example, Surratt et al (2007; 2010) found
253 that aerosol acidity can promote the formation of biogenic SOA (BSOA) derived from isoprene
254 oxidation such as 2-methylglyceric acid, Gly and mGly. These BSOA precursors can be further
255 oxidized into C₂ (Meng et al., 2014; Wang et al., 2009).

256 There is a significant positive correlation (R² = 0.58, *p*<0.001) between the mass ratios of
257 C₂/TDOC and ambient temperatures (Fig. 5f), which is similar to the results found by previous
258 researchers (Ho et al., 2007; Strader et al., 1999), indicating that organic aerosols are more aged
259 under a higher temperature condition (Erven et al, 2011; Carlton et al., 2009). Thus, compared
260 with those before-APEC the lower C₂/TDOC ratios (31% and 34%, respectively) (Fig. 4) during-
261 and after-APEC can be ascribed in part to the relatively lower temperature conditions that are not

262 favorable for oxidation of the precursors to produce oxalic acid (13 ± 2.6 °C, 7.0 ± 1.7 °C and
263 4.3 ± 1.3 °C before-, during- and after-APEC periods, respectively) (Table1).

264 **3.3.2 Temporal variation in stable carbon isotopic composition of oxalic acid**

265 To further discuss the formation mechanism of C_2 , we investigated the temporal variations
266 of concentration and stable carbon isotopic composition of C_2 in the $PM_{2.5}$ samples (Fig. 6).
267 Previous studies have demonstrated that Gly, mGly, glyoxylic acid (ωC_2) and pyruvic acid (Pyr)
268 are the precursors of C_2 (Carlton et al., 2006, 2007; Ervens and Barbara, 2004; Wang et al., 2012).
269 Thus, higher mass ratios of C_2 to its precursors indicate that organic aerosols are more oxidized
270 (Wang et al., 2010). As shown in Table 3, $\delta^{13}C$ of C_2 in this work positively correlated with the
271 mass ratios of $C_2/\omega C_2$, $C_2/mGly$ and TDOC/WSOC, demonstrating an enrichment of ^{13}C during
272 the aerosol oxidation process. Because decomposition (or breakdown) of larger molecular weight
273 precursors in aerosol aqueous phase is the dominant formation pathway for C_2 in aerosol ageing
274 process (Kawamura et al., 2016; Gensch et al., 2014; Kirillova et al., 2013), during which
275 organic compounds release CO_2/CO by reaction with OH radical and other oxidants, resulting in
276 the evolved species enriched with lighter isotope (^{12}C) and the remaining substrate enriched in
277 ^{13}C due to kinetic isotope effects (KIE) (Hoefs, 1997; Rudolph et al., 2002).

278 72-h backward trajectory analysis showed that air masses moved to Beijing during the
279 whole sampling period can roughly be categorized into three types (Fig. 6a) (all trajectories
280 during the entire study period can be found in the supplementary materials). (1) Polluted type, by
281 which air masses originated from inland and east coastal China and moved slowly into Beijing
282 within 72-h from its south regions, i.e., Henan, Shandong and Jiangsu provinces. This type of air
283 masses mostly occurred before-APEC with high $PM_{2.5}$ concentrations. Air pollution has widely

284 distributed in the three provinces (Wei et al., 2016); thus aerosols transported by this type of air
285 masses are of regional characteristics. (2) Mixed type, by which air masses originated from
286 Mongolia and North China, and moved quickly into Hebei province and then turned back to
287 Beijing. Air in Mongolia and North China was clean but polluted in Hebei province, which is
288 adjacent to Beijing. This type of air masses is a mixture of clean and polluted air and thus named
289 as mixed type. Since the resident time of the mixed type of air masses within Hebei province is
290 very short, thus aerosols transported by this type of air masses is of local characteristics and
291 relatively fresh. (3) Clean type, by which air masses originated from Siberia and moved rapidly
292 into Beijing directly via a long-range transport. Aerosols from the clean type of air masses are
293 much more aged, while those from the mixed type of air masses are fresh. Since severe air
294 pollution is widespread in the south regions, gas-to-aerosol phase partitioning of precursors and
295 subsequent aerosol-phase oxidation to produce SOA including C_2 continuously proceed during
296 the air mass movement. However, such a partition for producing SOA is not significant when air
297 mass move from Siberia, Mongolia and North China because of the much less abundant VOCs.
298 In stead, aerosols in the clean air masses are continuously oxidized, during which C_2 is produced
299 by photochemical decomposition of larger molecular weight precursors. Therefore, C_2 in $PM_{2.5}$
300 transported by the mixed type air masses are not only fresh and abundant but also enriched in ^{12}C ,
301 whereas C_2 in $PM_{2.5}$ transported by the clean type air masses are aged, less abundant and
302 enriched in ^{13}C due to KIE effects, as illustrated by the pink and light blue columns in Fig. 6b,
303 respectively. C_2 in $PM_{2.5}$ transported by the polluted type of air masses are most abundant
304 compared with that in other two types of air masses, which is not only due to the severe air
305 pollution in the Henan, Shandong and Jiangsu provinces but also due to the enhanced

306 photochemical oxidation under the humid, higher temperature and stagnant conditions that
307 occurred mostly before-APEC, as discussed previously. Therefore, C₂ in the polluted type of air
308 masses is not only abundant but also enriched in ¹³C (see black columns in Fig. 6b).

309 **3.4 Different chemical characteristics of PM_{2.5} between two severe haze events**

310 From Fig. 1 and Table 4, it can be found that PM_{2.5} showed two equivalent maxima on 9th
311 October and 20th November during the whole study period. However, the chemical compositions
312 of PM_{2.5} during these two pollution events are significantly different. As shown in Fig. 7a,
313 relative abundances of SIA (sum of SO₄²⁻, NO₃⁻ and NH₄⁺) to PM_{2.5} are 30% during the event I
314 and 23% during the event II, respectively. The relative abundance of OM (21%, Fig. 7a) during
315 the event I is lower than that (37%) during the event II (Fig. 7b). In contrast, the ratios of
316 WSOC/OC and TDOC/OC are higher in the event I than in the event II, which is consistent with
317 lower levels of O₃ after-APEC (Table 1), suggesting a weaker photochemical oxidation capacity
318 during the event II. Organic biomarkers in the PM_{2.5} samples have been measured for the source
319 apportionment (Wang et al., 2016) and cited here to further identify the difference in chemical
320 composition of PM_{2.5} between the two events. Levoglucosan is a key tracer for biomass burning
321 smoke. Mass ratio of levoglucosan to OC in PM_{2.5} (Lev/OC) is comparable between the two
322 events, suggesting a similar level of contributions of biomass burning emission to PM_{2.5} before-
323 and after-APEC. However, the mass ratios of PAHs and hopanes to OC are lower in event I than
324 those in event II (Fig. 7c), which again demonstrates the enhanced emissions from coal burning
325 for house heating, because these compounds are key tracers of coal burning smokes (Wang et al.,
326 2006). As seen in Fig. 7d, C₂ in the event I was enriched in ¹³C. Such relatively more abundant
327 SIA, WSOC and TDOC and heavier C₂ in PM_{2.5} clearly demonstrate that PM_{2.5} during the event

328 I are enriched with secondary products while the fine particles during the event II are enriched
329 with primary compounds. After-APEC house heating activities including residential coal burning
330 were activated, which emitted huge amounts of SO₂, NO_x, and VOCs as well as primary
331 particles, resulting in both absolute concentrations and relative abundances of CO and EC
332 30–40% higher after-APEC than before-APEC (see Table 1). Li et al (2015) reported that VOCs
333 in Beijing was 86 ppbv before-APEC, 48 ppbv during-APEC and 73 ppbv after-APEC. As
334 shown in Table 4, temperature (16.7±0.8 °C for event I and 4.5±1.7 °C for event II) and relative
335 humidity (RH) (82±4% for event I and 62±13% for event II) are lower during the event II than
336 during the event I. Moreover, air masses arriving in Beijing during the event II are the mix type,
337 of which the resident time in Hebei province is short. Compared with those in the event I, such
338 colder and drier conditions and short reaction time during the event II are unfavorable for
339 photochemical oxidation, resulting in SOA not only less abundant but also enriched with lighter
340 ¹²C during the event II, although VOCs levels are comparable before- and after-APEC.

341 **4. Summary and conclusion**

342 Temporal variations in molecular distribution of SIA, dicarboxylic acids, ketoacids and
343 α -dicarbonyl and stable carbon isotopic composition ($\delta^{13}\text{C}$) of C₂ in PM_{2.5} collected in Beijing
344 before-, during- and after- the 2014 APEC were investigated. Absolute concentrations and
345 relative abundances of SIA and C₂ in PM_{2.5} are highest before-APEC, followed by those after-
346 and during-APEC, suggesting that the fine aerosols before-APEC are enriched with secondary
347 products, mainly due to an enhanced photochemical oxidation under the warm, humid and
348 stagnant conditions. Concentrations of SIA, oxalic acid and related SOA in PM_{2.5} during-APEC
349 are 2–4 times lower than those before-APEC, which can be ascribed to the effective emission

350 controls and the favorable meteorological conditions that brought clean air from Siberia and
351 Mongolia into Beijing.

352 Positive correlations of C₂ with sulfate mass, RH, ALWC and aerosol acidity indicate that
353 C₂ formation pathway is involved an acid-catalyzed aerosol aqueous phase oxidation. SIA, C₂
354 and related SOA in the polluted type of air masses are abundant with C₂ enriched in ¹³C. On the
355 contrary, those in the clean type of air masses are much less abundant, although C₂ is also
356 enriched in ¹³C. By comparing the chemical composition of PM_{2.5} and δ¹³C values of C₂ in two
357 events that are characterized by the highest loadings of PM_{2.5} before- and after-APEC, we further
358 found that compared with those before- APEC fine aerosols after-APEC are enriched with
359 primary species and C₂ is depleted in heavier ¹³C, although SO₂, NO_x and VOCs are abundant
360 during the heating season, again demonstrating the important role of meteorological conditions
361 in the secondary aerosol formation process, which are warmer, humid and stagnant before-APEC
362 and result in secondary species much more abundant than those during- and after-APEC.

363

364 **Acknowledgements**

365 This work was financially supported by the Strategic Priority Research Program of the
366 Chinese Academy of Sciences (Grants No. XDB05020401), the China National Natural Science
367 Funds for Distinguished Young Scholars (Grants No. 41325014), and the program from
368 National Nature Science Foundation of China (No. 41405122, 91544226 and 41375132).

369

370

371 **References**

- 372 Bikkina, S., Kawamura, K., and Miyazaki, Y.: Latitudinal distributions of atmospheric dicarboxylic acids,
373 oxocarboxylic acids, and α-dicarbonyls over the western North Pacific: Sources and formation pathways, *Journal*
374 *of Geophysical Research: Atmospheres*, 120, 5010-5035, 10.1002/2014jd022235, 2015.
- 375 Carlton, A. G., Turpin, B. J., Lim, H.-J., Altieri, K. E., and Seitzinger, S.: Link between isoprene and secondary
376 organic aerosol (SOA): Pyruvic acid oxidation yields low volatility organic acids in clouds, *Geophysical*
377 *Research Letters*, 33, 10.1029/2005gl025374, 2006.

378 Carlton, A. G., Turpin, B. J., Altieri, K. E., Seitzinger, S., Reff, A., Lim, H.-J., and Ervens, B.: Atmospheric oxalic
379 acid and SOA production from glyoxal: Results of aqueous photooxidation experiments, *Atmospheric*
380 *Environment*, 41, 7588-7602, 10.1016/j.atmosenv.2007.05.035, 2007.

381 Carlton, A., Wiedinmyer, C., and Kroll, J.: A review of Secondary Organic Aerosol (SOA) formation from isoprene,
382 *Atmospheric Chemistry and Physics*, 9, 4987-5005, 2009.

383 Cheng, C., Wang, G., Meng, J., Wang, Q., Cao, J., Li, J., and Wang, J.: Size-resolved airborne particulate oxalic and
384 related secondary organic aerosol species in the urban atmosphere of Chengdu, China, *Atmospheric Research*,
385 161-162, 134-142, 10.1016/j.atmosres.2015.04.010, 2015.

386 Chow, J. C., Watson, J. G., Chen, L.-W. A., Chang, M. O., Robinson, N. F., Trimble, D., and Kohl, S.: The
387 IMPROVE_A temperature protocol for thermal/optical carbon analysis: maintaining consistency with a
388 long-term database, *Journal of the Air & Waste Management Association*, 57, 1014-1023, 2007.

389 Ervens, B.: A modeling study of aqueous production of dicarboxylic acids: 1. Chemical pathways and speciated
390 organic mass production, *Journal of Geophysical Research*, 109, 10.1029/2003jd004387, 2004.

391 Ervens, B., Turpin, B. J., and Weber, R. J.: Secondary organic aerosol formation in cloud droplets and aqueous
392 particles (aqSOA): a review of laboratory, field and model studies, *Atmospheric Chemistry and Physics*, 11,
393 11069-11102, 10.5194/acp-11-11069-2011, 2011.

394 Fu, T.-M., Jacob, D. J., Wittrock, F., Burrows, J. P., Vrekoussis, M., and Henze, D. K.: Global budgets of
395 atmospheric glyoxal and methylglyoxal, and implications for formation of secondary organic aerosols, *Journal of*
396 *Geophysical Research*, 113, 10.1029/2007jd009505, 2008.

397 Gensch, I., Kiendler-Scharr, A., and Rudolph, J.: Isotope ratio studies of atmospheric organic compounds: Principles,
398 methods, applications and potential, *International Journal of Mass Spectrometry*, 365-366, 206-221,
399 10.1016/j.ijms.2014.02.004, 2014.

400 Guo, S., Hu, M., Zamora, M. L., Peng, J., Shang, D., Zheng, J., Du, Z., Wu, Z., Shao, M., Zeng, L., Molina, M. J.,
401 and Zhang, R.: Elucidating severe urban haze formation in China, *Proceedings of the National Academy of*
402 *Sciences of the United States of America*, 111, 17373-17378, 10.1073/pnas.1419604111, 2014.

403 Hennigan, C. J., Izumi, J., Sullivan, A. P., Weber, R. J., and Nenes, A.: A critical evaluation of proxy methods used
404 to estimate the acidity of atmospheric particles, *Atmospheric Chemistry and Physics*, 15, 2775-2790,
405 10.5194/acp-15-2775-2015, 2015.

406 Ho, K. F., Cao, J. J., Lee, S. C., Kawamura, K., Zhang, R. J., Chow, J. C., and Watson, J. G.: Dicarboxylic acids,
407 ketocarboxylic acids, and dicarbonyls in the urban atmosphere of China, *Journal of Geophysical Research*, 112,
408 10.1029/2006jd008011, 2007.

409 Ho, K. F., Lee, S. C., Ho, S. S. H., Kawamura, K., Tachibana, E., Cheng, Y., and Zhu, T.: Dicarboxylic acids,
410 ketocarboxylic acids, α -dicarbonyls, fatty acids, and benzoic acid in urban aerosols collected during the 2006
411 Campaign of Air Quality Research in Beijing (CAREBeijing-2006), *Journal of Geophysical Research*, 115,
412 10.1029/2009jd013304, 2010.

413 Ho, K. F., Huang, R. J., Kawamura, K., Tachibana, E., Lee, S. C., Ho, S. S. H., Zhu, T., and Tian, L.: Dicarboxylic
414 acids, ketocarboxylic acids, α -dicarbonyls, fatty acids and benzoic acid in PM_{2.5} aerosol collected
415 during CAREBeijing-2007: an effect of traffic restriction on air quality, *Atmospheric Chemistry and Physics*, 15,
416 3111-3123, 10.5194/acp-15-3111-2015, 2015.

417 Hoefs, J., and Hoefs, J.: *Stable isotope geochemistry*, Springer, 1997.

418 Huang, R. J., Zhang, Y., Bozzetti, C., Ho, K. F., Cao, J. J., Han, Y., Daellenbach, K. R., Slowik, J. G., Platt, S. M.,
419 Canonaco, F., Zotter, P., Wolf, R., Pieber, S. M., Bruns, E. A., Crippa, M., Ciarelli, G., Piazzalunga, A.,
420 Schwikowski, M., Abbazade, G., Schnelle-Kreis, J., Zimmermann, R., An, Z., Szidat, S., Baltensperger, U., El

421 Haddad, I., and Prevot, A. S.: High secondary aerosol contribution to particulate pollution during haze events in
422 China, *Nature*, 514, 218-222, 10.1038/nature13774, 2014.

423 Kawamura, K., and Watanabe, T.: Determination of stable carbon isotopic compositions of low molecular weight
424 dicarboxylic acids and ketocarboxylic acids in atmospheric aerosol and snow samples, *Analytical Chemistry*, 76,
425 5762-5768, 2004.

426 Kawamura, K., and Bikkina, S.: A review of dicarboxylic acids and related compounds in atmospheric aerosols:
427 Molecular distributions, sources and transformation, *Atmospheric Research*, 170, 140-160,
428 <http://dx.doi.org/10.1016/j.atmosres.2015.11.018>, 2016.

429 Kirillova, E. N., Andersson, A., Sheesley, R. J., Kruså, M., Praveen, P. S., Budhavant, K., Safai, P. D., Rao, P. S. P.,
430 and Gustafsson, Ö.: 13C- and 14C-based study of sources and atmospheric processing of water-soluble organic
431 carbon (WSOC) in South Asian aerosols, *Journal of Geophysical Research: Atmospheres*, 118, 614-626,
432 10.1002/jgrd.50130, 2013.

433 Laskin, A., Laskin, J., and Nizkorodov, S. A.: Chemistry of Atmospheric Brown Carbon, *Chemical reviews*, 115,
434 4335-4382, 10.1021/cr5006167, 2015.

435 Li, J., Xie, S. D., Zeng, L. M., Li, L. Y., Li, Y. Q., and Wu, R. R.: Characterization of ambient volatile organic
436 compounds and their sources in Beijing, before, during, and after Asia-Pacific Economic Cooperation China
437 2014, *Atmospheric Chemistry and Physics*, 15, 7945-7959, 10.5194/acp-15-7945-2015, 2015.

438 Li, W., and Shao, L.: Mixing and water-soluble characteristics of particulate organic compounds in individual urban
439 aerosol particles, *Journal of Geophysical Research*, 115, 10.1029/2009jd012575, 2010.

440 Li, W., Zhou, S., Wang, X., Xu, Z., Yuan, C., Yu, Y., Zhang, Q., and Wang, W.: Integrated evaluation of aerosols
441 from regional brown hazes over northern China in winter: Concentrations, sources, transformation, and mixing
442 states, *Journal of Geophysical Research*, 116, 10.1029/2010jd015099, 2011.

443 Ma, Y., Brooks, S. D., Vidaurre, G., Khalizov, A. F., Wang, L., and Zhang, R.: Rapid modification of
444 cloud-nucleating ability of aerosols by biogenic emissions, *Geophysical Research Letters*, 40, 6293-6297,
445 10.1002/2013gl057895, 2013.

446 Meng, J., Wang, G., Li, J., Cheng, C., Ren, Y., Huang, Y., Cheng, Y., Cao, J., and Zhang, T.: Seasonal
447 characteristics of oxalic acid and related SOA in the free troposphere of Mt. Hua, central China: implications for
448 sources and formation mechanisms, *Sci Total Environ*, 493, 1088-1097, 10.1016/j.scitotenv.2014.04.086, 2014.

449 Mu Q., and Zhang. S.: An evaluation of the economic loss due to the heavy haze during January 2013 in China.,
450 *China Environmental Science*, 33, 2087-2094, 2013.

451 Myriokefalitakis, S., Tsigaridis, K., Mihalopoulos, N., Sciare, J., Nenes, A., Kawamura, K., Segers, A., and
452 Kanakidou, M.: In-cloud oxalate formation in the global troposphere: a 3-D modeling study, *Atmospheric
453 Chemistry and Physics*, 11, 5761-5782, 2011.

454 Peng, J., Hu, M., Guo, S., Du, Z., Zheng, J., Shang, D., Zamora, M. L., Zeng, L., Shao, M., and Wu, Y.-S.:
455 Markedly enhanced absorption and direct radiative forcing of black carbon under polluted urban environments,
456 *Proceedings of the National Academy of Sciences*, 113, 4266-4271, 2016.

457 Rudolph, J., Czuba, E., Norman, A., Huang, L., and Ernst, D.: Stable carbon isotope composition of nonmethane
458 hydrocarbons in emissions from transportation related sources and atmospheric observations in an urban
459 atmosphere, *Atmospheric Environment*, 36, 1173-1181, 2002.

460 Sorooshian, A., Lu, M.-L., Brechtel, F. J., Jonsson, H., Feingold, G., Flagan, R. C., and Seinfeld, J. H.: On the
461 Source of Organic Acid Aerosol Layers above Clouds, *Environmental Science & Technology*, 41, 4647-4654,
462 10.1021/es0630442, 2007.

463 Strader, R., Lurmann, F., and Pandis, S. N.: Evaluation of secondary organic aerosol formation in winter,
464 *Atmospheric Environment*, 33, 4849-4863, 1999.

465 Sullivan, R. C., and Prather, K. A.: Investigations of the Diurnal Cycle and Mixing State of Oxalic Acid in
466 Individual Particles in Asian Aerosol Outflow, *Environmental Science & Technology*, 41, 8062-8069,
467 10.1021/es071134g, 2007.

468 Sun, Y., Wang, Z., Wild, O., Xu, W., Chen, C., Fu, P., Du, W., Zhou, L., Zhang, Q., Han, T., Wang, Q., Pan, X.,
469 Zheng, H., Li, J., Guo, X., Liu, J., and Worsnop, D. R.: "APEC Blue": Secondary Aerosol Reductions from
470 Emission Controls in Beijing, *Scientific reports*, 6, 20668, 10.1038/srep20668, 2016.

471 Surratt, J. D., Lewandowski, M., Offenberg, J. H., Jaoui, M., Kleindienst, T. E., Edney, E. O., and Seinfeld, J. H.:
472 Effect of acidity on secondary organic aerosol formation from isoprene, *Environmental Science & Technology*,
473 41, 5363-5369, 2007.

474 Surratt, J. D., Chan, A. W., Eddingsaas, N. C., Chan, M., Loza, C. L., Kwan, A. J., Hersey, S. P., Flagan, R. C.,
475 Wennberg, P. O., and Seinfeld, J. H.: Reactive intermediates revealed in secondary organic aerosol formation
476 from isoprene, *Proceedings of the National Academy of Sciences*, 107, 6640-6645, 2010.

477 Tang, G., Zhu, X., Hu, B., Xin, J., Wang, L., Munkel, C., Mao, G., and Wang, Y.: Impact of emission controls on
478 air quality in Beijing during APEC 2014: lidar ceilometer observations, *Atmospheric Chemistry and Physics*, 15,
479 12667-12680, 2015.

480 Tilgner, A., and Herrmann, H.: Radical-driven carbonyl-to-acid conversion and acid degradation in tropospheric
481 aqueous systems studied by CAPRAM, *Atmospheric Environment*, 44, 5415-5422, 2010.

482 van Donkelaar, A., Martin, R. V., Brauer, M., Kahn, R., Levy, R., Verduzco, C., and Villeneuve, P. J.: Global
483 Estimates of Ambient Fine Particulate Matter Concentrations from Satellite-Based Aerosol Optical Depth:
484 Development and Application, *Environmental Health Perspectives*, 118, 847-855, 10.1289/ehp.0901623, 2010.

485 van Pinxteren, D., Neusüß, C., and Herrmann, H.: On the abundance and source contributions of dicarboxylic acids
486 in size-resolved aerosol particles at continental sites in central Europe, *Atmospheric Chemistry and Physics*, 14,
487 3913-3928, 10.5194/acp-14-3913-2014, 2014.

488 Wang, G., Niu, S., Liu, C., and Wang, L.: Identification of dicarboxylic acids and aldehydes of PM10 and PM2.5
489 aerosols in Nanjing, China, *Atmospheric Environment*, 36, 1941-1950, 2002.

490 Wang, G., Kawamura, K., Lee, S., Ho, K., and Cao, J.: Molecular, seasonal, and spatial distributions of organic
491 aerosols from fourteen Chinese cities, *Environmental Science & Technology*, 40, 4619-4625, 2006.

492 Wang, G., Kawamura, K., Umemoto, N., Xie, M., Hu, S., and Wang, Z.: Water-soluble organic compounds in
493 PM2.5 and size-segregated aerosols over Mount Tai in North China Plain, *Journal of Geophysical Research*, 114,
494 10.1029/2008jd011390, 2009.

495 Wang, G., Xie, M., Hu, S., Gao, S., Tachibana, E., and Kawamura, K.: Dicarboxylic acids, metals and isotopic
496 compositions of C and N in atmospheric aerosols from inland China: implications for dust and coal burning
497 emission and secondary aerosol formation, *Atmospheric Chemistry and Physics*, 10, 6087-6096,
498 10.5194/acp-10-6087-2010, 2010.

499 Wang, G., Kawamura, K., Cheng, C., Li, J., Cao, J., Zhang, R., Zhang, T., Liu, S., and Zhao, Z.: Molecular
500 distribution and stable carbon isotopic composition of dicarboxylic acids, ketocarboxylic acids, and
501 alpha-dicarbonyls in size-resolved atmospheric particles from Xi'an City, China, *Environ Sci Technol*, 46,
502 4783-4791, 10.1021/es204322c, 2012.

503 Wang, G., Cheng, C., Meng, J., Huang, Y., Li, J., and Ren, Y.: Field observation on secondary organic aerosols
504 during Asian dust storm periods: Formation mechanism of oxalic acid and related compounds on dust surface,
505 *Atmospheric Environment*, 113, 169-176, 10.1016/j.atmosenv.2015.05.013, 2015a.

506 Wang, G., Wang, J., Ren, Y. and Li, J.: Chemical characterization of organic aerosols from Beijing during the 2014
507 APEC (under preparation), 2016.

508 Wang, G., Zhang, R., Gomez, M. E., Yang, L., Levy Zamora, M., Hu, M., Lin, Y., Peng, J., Guo, S., Meng, J., Li, J.,
509 Cheng, C., Hu, T., Ren, Y., Wang, Y., Gao, J., Cao, J., An, Z., Zhou, W., Li, G., Wang, J., Tian, P.,
510 Marrero-Ortiz, W., Secrest, J., Du, Z., Zheng, J., Shang, D., Zeng, L., Shao, M., Wang, W., Huang, Y., Wang, Y.,
511 Zhu, Y., Li, Y., Hu, J., Pan, B., Cai, L., Cheng, Y., Ji, Y., Zhang, F., Rosenfeld, D., Liss, P. S., Duce, R. A.,
512 Kolb, C. E., and Molina, M. J.: Persistent sulfate formation from London Fog to Chinese haze, *Proceedings of*
513 *the National Academy of Sciences*, 113, 13630-13635, 10.1073/pnas.1616540113, 2016.

514 Wang, Z., Li, Y., Chen, T., Li, L., Liu, B., Zhang, D., Sun, F., Wei, Q., Jiang, L., and Pan, L.: Changes in
515 atmospheric composition during the 2014 APEC conference in Beijing, *Journal of Geophysical Research:*
516 *Atmospheres*, 120, 12695-12707, 10.1002/2015JD023652, 2015b.

517 Weber, R. J., Guo, H., Russell, A. G., and Nenes, A.: High aerosol acidity despite declining atmospheric sulfate
518 concentrations over the past 15 years, *Nature Geoscience*, 9, 282-285, 10.1038/ngeo2665, 2016.

519 Wei, X., Gu, X., Chen, H., Cheng, T., Wang, Y., Guo, H., Bao, F., and Xiang, K.: Multi-Scale Observations of
520 Atmosphere Environment and Aerosol Properties over North China during APEC Meeting Periods, *Atmosphere*,
521 7, 4, 2015.

522 Xing, L., Fu, T. M., Cao, J. J., Lee, S. C., Wang, G. H., Ho, K. F., Cheng, M. C., You, C. F., and Wang, T. J.:
523 Seasonal and spatial variability of the OM/OC mass ratios and high regional correlation between oxalic acid and
524 zinc in Chinese urban organic aerosols, *Atmospheric Chemistry and Physics*, 13, 4307-4318,
525 10.5194/acp-13-4307-2013, 2013.

526 Xu, W. Q., Sun, Y. L., Chen, C., Du, W., Han, T. T., Wang, Q. Q., Fu, P. Q., Wang, Z. F., Zhao, X. J., Zhou, L. B.,
527 Ji, D. S., Wang, P. C., and Worsnop, D. R.: Aerosol composition, oxidation properties, and sources in Beijing:
528 results from the 2014 Asia-Pacific Economic Cooperation summit study, *Atmospheric Chemistry and Physics*,
529 15, 13681-13698, 10.5194/acp-15-13681-2015, 2015.

530 Xue, H., Khalizov, A. F., Wang, L., Zheng, J., and Zhang, R.: Effects of coating of dicarboxylic acids on the mass-
531 mobility relationship of soot particles, *Environmental science & technology*, 43, 2787-2792, 2009.

532 Yu, J. Z., Huang, X.-F., Xu, J., and Hu, M.: When Aerosol Sulfate Goes Up, So Does Oxalate: Implication for the
533 Formation Mechanisms of Oxalate, *Environmental Science & Technology*, 39, 128-133, 10.1021/es049559f,
534 2005.

535 Zhang, R., Suh, I., Zhao, J., Zhang, D., Fortner, E. C., Tie, X., Molina, L. T., and Molina, M. J.: Atmospheric new
536 particle formation enhanced by organic acids, *Science*, 304, 1487-1490, 10.1126/science.1095139, 2004.

537 Zhang, Q., Jimenez, J. L., Worsnop, D. R., and Canagaratna, M.: A case study of urban particle acidity and its
538 influence on secondary organic aerosol, *Environmental science & technology*, 41, 3213-3219, 2007.

539 Zhang, R., Khalizov, A., Wang, L., Hu, M., and Xu, W.: Nucleation and growth of nanoparticles in the atmosphere,
540 *Chemical reviews*, 112, 1957-2011, 10.1021/cr2001756, 2012.

541 Zhang, R., Wang, G., Guo, S., Zamora, M. L., Ying, Q., Lin, Y., Wang, W., Hu, M., and Wang, Y.: Formation of
542 urban fine particulate matter, *Chemical reviews*, 115, 3803-3855, 10.1021/acs.chemrev.5b00067, 2015.

543 Zhao, J., Khalizov, A., Zhang, R., and McGraw, R.: Hydrogen-bonding interaction in molecular complexes and
544 clusters of aerosol nucleation precursors, *The Journal of Physical Chemistry A*, 113, 680-689, 2009.

545
546
547
548
549
550
551

Figure Captions

552

553

554 **Figure 1.** Temporal variations of meteorological conditions, gaseous pollutants and major
555 components of PM_{2.5} during the 2014 APEC campaign. (The brown shadows
556 represent two air pollution events characterized by highest PM_{2.5} levels before- and
557 after-APEC, while the blue shadow represents the APEC event).

558

559 **Figure 2.** Chemical composition of PM_{2.5} during the 2014 APEC campaign.

560

561 **Figure 3.** Molecular distributions of dicarboxylic acids and related compounds in PM_{2.5} of
562 Beijing, China during the 2014 APEC campaign. The pie chart is the average
563 composition of total detected organic compounds (TDOC) and the top number is the
564 average mass concentration of TDOC of the whole study period.

565

566 **Figure 4.** Compositions of total detected organic compounds (TDOC) in PM_{2.5} during the 2014
567 APEC campaign.

568

569 **Figure 5.** Correlation analysis for oxalic acid (C₂) and sulfate in PM_{2.5} during the whole 2014
570 APEC campaign. **(a-c)** Concentrations of C₂ with sulfate, relative humidity (RH), and
571 aerosol liquid water content (ALWC); **(d, e)** sulfate and C₂ with aerosol acidity [H⁺]
572 and **(f)** temperature with mass ratio of C₂ to total detected organic compounds
573 (C₂/TDOC).

574

575 **Figure 6.** **(a)** 72-h backward trajectories determined by the National Oceanic and Atmospheric
576 Administration Hybrid Single Particle Lagrangian Integrated Trajectory (HYSPLIT)
577 model arriving at the sampling site to reveal the major air mass flow types during the
578 study period. Northwesterly wind (light blue) was most frequently (64%), followed by
579 northerly (21%, pink) and southerly (15%, black) and is defined as clean, mixed and
580 polluted types, respectively (see the definitions in the text and the trajectories with a
581 6-hr interval in the supplementary section); **(b)** Time series of δ¹³C values and
582 concentration of oxalic acid during the whole study period (Colors in Fig. 6a are
583 corresponding to those in Fig. 6b).

584

585 **Figure 7.** Comparison of chemical composition of PM_{2.5} during two air pollution events. **(a)**
586 Percentages of major species in PM_{2.5}; **(b, c)** mass ratios of major species and organic
587 tracers in PM_{2.5}; **(d)** stable carbon isotope composition of oxalic acid (C₂) (Data about
588 levoglucosan (Lev), PAHs and hopanes are cited from Wang et al (2016)).

589

590

591
592
593
594
595
596
597
598
599
600
601
602
603
604
605
606
607
608
609
610
611
612
613
614
615
616
617

Table 1. Meteorological parameters and concentrations of gaseous pollutants and chemical components of PM_{2.5} in Beijing during the 2014 APEC campaign

	Whole period (N=48)	Before-APEC (08/10–02/11) (N=26)	During-APE (03/11–12/11) (N=10)	After-APEC (13/11–14/11) (N=12)
I. Meteorological parameters				
Temperature, °C	9.5±4.3 (3.0–18)	13±2.6 (9.0–18)	7.0±1.7 (4.0–10)	4.3±1.3 (3.0–7.0)
Relative humidity,	56±19 (17–88)	62±19 (22–88)	47±14 (17–65)	51±16 (29–80)
Visibility, km	8.8±6.8 (1.0–28)	7.3±6.6 (1.0–24)	13±7.7 (6.0–28)	7.2±4.2 (2.0–15)
Wind speed, km	8.0±4.9 (3.0–26)	7.6±4.8 (3.0–26)	9.4±6.6 (3.0–26)	7.8±2.9 (3.0–13)
II. Gaseous pollutants, µg m ⁻³				
O ₃	48 ± 23 (6.0–115)	55 ± 24 (9.0–115)	52 ± 13 (25–69)	29 ± 18 (6.0–60)
SO ₂	12 ± 8.5 (2.0–43)	8.8 ± 4.6 (2.0–19)	7.6 ± 3.9 (2.0–15)	23 ± 8.8 (13–43)
NO ₂	68 ± 29 (10–135)	71 ± 27 (22–118)	45 ± 18 (10–69)	78 ± 29 (45–135)
CO	1360 ± 730 (220–3320)	1370 ± 700 (250–2460)	960 ± 410 (220–1420)	1720 ± 830 (740–3320)
III. Major components of PM _{2.5} , µg m ⁻³				
PM _{2.5}	157 ± 110 (16–408)	178 ± 122 (16–408)	98 ± 46 (28–183)	161 ± 100 (36–383)
SO ₄ ²⁻	12 ± 11.5 (1.2–43)	15 ± 13 (1.2–43)	5.3 ± 2.8 (1.8–11)	11 ± 10 (2.9–34)
NO ₃ ⁻	21 ± 22 (0.32–88)	28 ± 26 (0.32–88)	10 ± 8.1 (1.2–26)	15 ± 13 (2.9–46)
NH ₄ ⁺	7.3±7.2 (0.2–28)	9.0 ± 8.0 (0.2–28)	3.1 ± 2.6 (0.2–8.6)	6.9 ± 6.4 (1.0–22)
OC ^a	28 ± 18 (5.7–78)	26 ± 16 (6.0–67)	19 ± 7.6 (5.7–29)	39 ± 23 (9.7–78)
EC ^a	8.8 ± 5.4 (1.4–25)	8.6 ± 4.6 (1.4–18)	6.0 ± 2.7 (1.5–9.6)	12 ± 7.0 (2.1–25)
WSOC ^b	10 ± 6.0 (2.4–32)	11 ± 4.6 (3.1–32)	6.4 ± 2.6 (2.4–11)	11 ± 6.1 (4.5–24)
ALWC ^c	40 ± 62 (0–299)	58 ± 75 (0–299)	6.3 ± 5.5 (0–19)	28 ± 41 (0.4–136)
[H ⁺] ^d	0.083 ± 0.14 (0–0.56)	0.13 ± 0.17 (0–0.56)	0.026 ± 0.025 (0–0.072)	0.033 ± 0.067 (0–0.20)
IV. Mass ratios of major components of PM _{2.5}				
NO ₃ ⁻ /SO ₄ ²⁻	1.6±0.8 (0.3–4.3)	1.7±0.9 (0.3–4.3)	1.6±0.7 (0.5–2.4)	1.4±0.4 (0.8–2.2)
OC/EC	3.3±0.6 (2.2–4.7)	3.2±0.7 (2.2–4.5)	3.3±0.6 (2.0–4.3)	3.4±0.5 (2.7–4.7)
WSOC/OC	0.39±0.15 (0.10–0.71)	0.42±0.13 (0.13–0.71)	0.38±0.16 (0.16–0.65)	0.35±0.17 (0.10–0.63)

^aOrganic (OC) and elemental carbon (EC); ^bWater-soluble organic carbon (WSOC); ^cAerosol liquid water content (ALWC); ^dHydrogen ion concentration ([H⁺])

Table 2. Concentrations of dicarboxylic acids and related compounds in PM_{2.5} in Beijing during the 2014 APEC campaign (ng m⁻³)

	Whole period (N=48)	Before-APEC (08/10–02/11) (N=26)	During-APE (03/11–12/11) (N=10)	After-APEC (13/11–14/11) (N=12)
I. Dicarboxylic acids				
Oxalic, C ₂	334 ± 461 (10–2127)	502 ± 564 (10.5–2127)	101 ± 69 (35–251)	166 ± 157 (22–554)
Malonic, C ₃	31 ± 42 (ND–247)	45.7 ± 52.1 (1.44–247)	12 ± 8.0 (3.4–22.8)	16 ± 10.9 (ND–36)
Succinic, C ₄	74 ± 118 (3.0–722)	111 ± 150 (3.0–722)	24 ± 14 (7.1–42)	36 ± 26 (4.9–90)
Glutaric, C ₅	8.7 ± 12 (ND–68)	13 ± 15 (ND–68.1)	2.9 ± 2.24 (0.9–5.8)	4.9 ± 4.2 (ND–13)
Adipic, C ₆	13 ± 14 (0.9–83)	17 ± 18 (1.9–83)	5.9 ± 3.8 (2.1–14)	9.9 ± 7.1 (2.0–23)
Pimelic, C ₇	2.1 ± 3.8 (ND–27)	2.6 ± 5.1 (ND–27)	1.1 ± 0.7 (0.2–2.3)	2.0 ± 1.1 (0.9–4.4)
Suberic, C ₈	10 ± 11 (ND–66)	12 ± 13 (ND–66)	7.6 ± 5.0 (1.3–16)	8.7 ± 6.0 (2.0–21)
Azelaic, C ₉	5.0 ± 4.9 (0.5–21)	6.4 ± 5.7 (0.6–21)	1.7 ± 0.9 (0.5–3.2)	4.6 ± 3.3 (1.3–13)
Sebacic, C ₁₀	7.7 ± 7.4 (ND–34)	9.4 ± 8.8 (ND–34)	4.2 ± 3.6 (0.5–11)	6.8 ± 4.9 (1.4–16)
Undecanedioic, C ₁₁	11 ± 13 (ND–77)	14 ± 16 (ND–77)	3.3 ± 2.5 (ND–7.5)	9.4 ± 6.4 (0.8–23)
Methylsuccinic, iC ₅	13 ± 16 (0.6–79)	18 ± 19 (0.6–79)	4.8 ± 3.0 (1.0–9.2)	8.4 ± 6.0 (2.3–19)
Methylglutaric, iC ₆	7.5 ± 10 (ND–36)	11 ± 12 (ND–36)	0.9 ± 0.9 (ND–2.6)	4.6 ± 5.1 (ND–14)
Maleic, M	3.4 ± 3.9 (ND–15)	4.6 ± 4.7 (ND–15)	1.4 ± 0.8 (ND–2.9)	2.4 ± 2.0 (ND–6.3)
Fumaric, F	7.2 ± 8.8 (ND–64)	10 ± 11 (ND–64)	2.2 ± 1.5 (ND–5.4)	4.7 ± 3.2 (1.4–10)
Phthalic, Ph	17 ± 14 (1.5–64)	20 ± 16 (1.5–64)	10 ± 6.8 (2.3–20)	17 ± 9.0 (6.4–31)
Isophthalic, iPh	2.1 ± 2.5 (ND–10)	2.9 ± 2.8 (ND–10)	2.0 ± 2.1 (0.2–5.9)	0.5 ± 0.3 (ND–3.2)
Terephthalic, tPh	46 ± 35 (2.6–133)	50 ± 35 (2.6–123)	28 ± 19 (4.7–59)	53 ± 40 (7.4–133)
Subtotal	593 ± 739 (25–3788)	849 ± 905 (25–3788)	214 ± 135 (72–447)	354 ± 279 (85–965)
II. Keto-carboxylic acids				
Pyruvic, Pyr	24 ± 20 (1.3–84)	31 ± 23 (2.4–84)	15 ± 12 (1.3–36)	15 ± 9.3 (3.2–33)
Glyoxylic, ωC ₂	33 ± 51 (1.2–300)	48 ± 64 (1.2–300)	10 ± 7.7 (2.6–21)	20 ± 23 (2.8–80)
7-Oxoheptanoic, ωC ₇	8.8 ± 14 (ND–90)	13 ± 17 (ND–90)	4.2 ± 3.6 (ND–13)	4.5 ± 5.1 (ND–17)
Subtotal	66 ± 81 (3.6–474)	92 ± 99 (3.6–474)	30 ± 22 (5.9–66)	40 ± 35 (13–128)
III α-Dicarbonyls				
Glyoxal, Gly	44 ± 47 (4.2–270)	57 ± 56 (4.2–270)	22 ± 19 (4.9–47)	35 ± 30 (7.3–101)
Methylglyoxal, mGly	82 ± 82 (ND–406)	102 ± 96 (ND–406)	60 ± 52 (15–139)	58 ± 51 (5.8–144)
Subtotal	126 ± 115 (5.3–466)	158 ± 132 (5.3–466)	81.6 ± 67.4 (22–186)	93 ± 80 (14–225)
TDOC ^b	785 ± 872 (36–4636)	1099 ± 1104 (36–4636)	325 ± 220 (107–664)	487 ± 387 (117–1318)

^aND: not detectable; ^bTDOC: total detected organic compounds.

620
621
622
623

Table 3 Linear correlation coefficients of $\delta^{13}\text{C}$ of C_2 with $\text{C}_2/\omega\text{C}_2$, C_2/mGly , and TDOC/WSOC

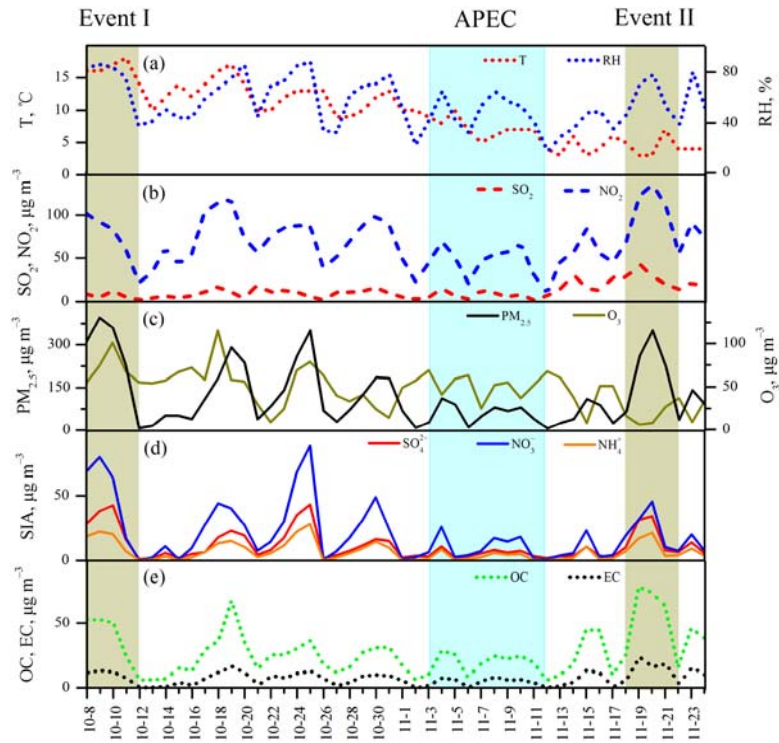
	$\text{C}_2/\omega\text{C}_2$	C_2/mGly	TDOC/WSOC
$\delta^{13}\text{C}$	0.49**	0.35*	0.41*

** $p < 0.01$; * $p < 0.05$

Table 4. Meteorological parameters and chemical compositions ($\mu\text{g m}^{-3}$) of two maximum $\text{PM}_{2.5}$ between two pollution episodes in Beijing

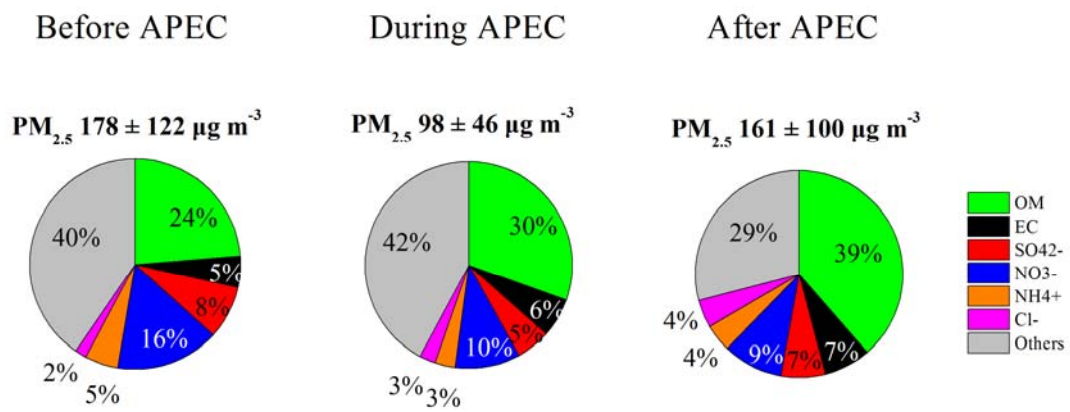
	T ($^{\circ}\text{C}$)	RH (%)	V ^a (km)	$\text{PM}_{2.5}$	OC	EC	SIA ^b	TDOC ^c
Event I (8/10-11/10, Before-APEC)	16.7 ± 0.8	82 ± 4	1.5 ± 0.5	349 ± 57	45 ± 12	12 ± 2	106 ± 39	2749 ± 1357
Event II (18/11-21/11, After-APEC)	4.5 ± 1.7	62 ± 13	3.5 ± 1.5	259 ± 102	60 ± 21	17 ± 6	60 ± 32	831 ± 400

^aV: visibility; ^bSIA: secondary inorganic ions (the sum of sulfate, nitrate and ammonium); ^cTDOC: total detected organic compounds



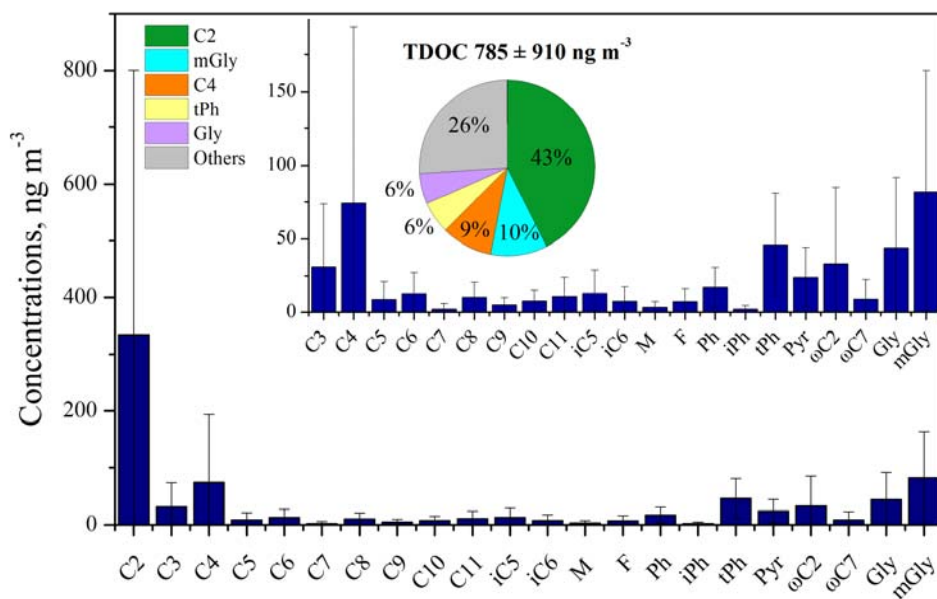
627

628 **Figure 1.** Temporal variations of meteorological conditions, gaseous pollutants and major components of $PM_{2.5}$
 629 during the 2014 APEC campaign. (The brown shadows represent two air pollution events characterized
 630 by highest $PM_{2.5}$ levels before- and after-APEC, while the blue shadow represents the APEC event).



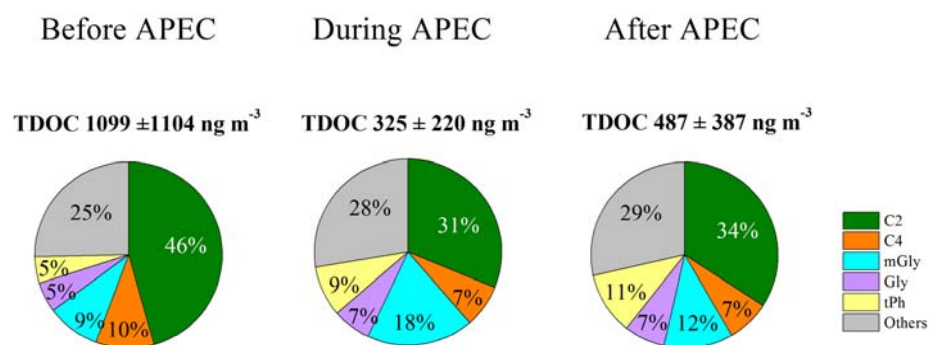
631
632
633

Figure 2. Chemical composition of $PM_{2.5}$ during the 2014 APEC campaign.



635

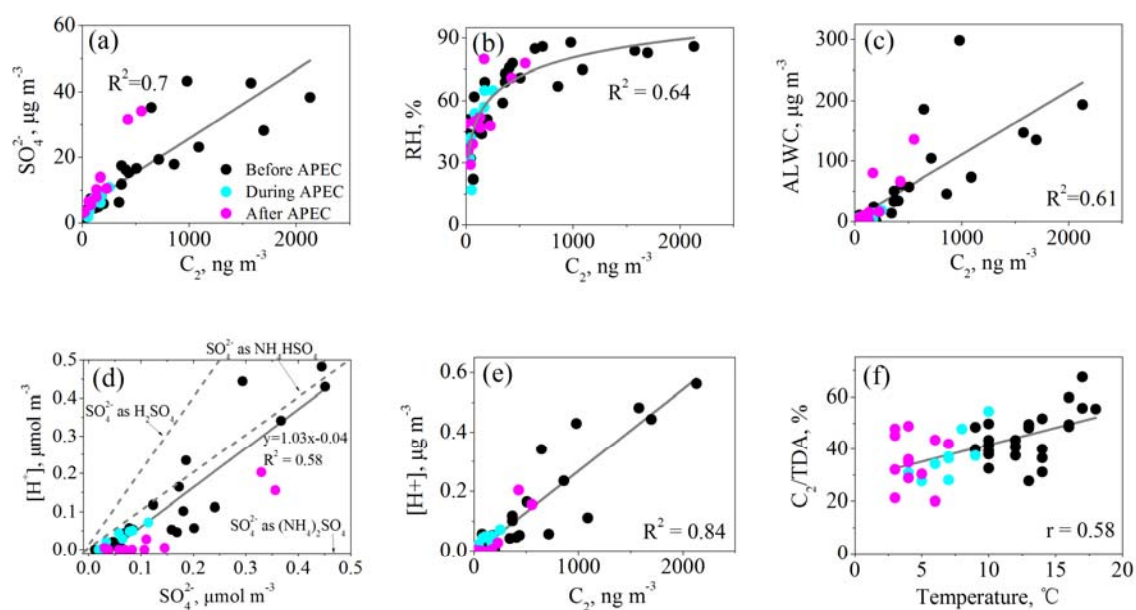
636 **Figure 3.** Molecular distributions of dicarboxylic acids and related compounds in $\text{PM}_{2.5}$ of Beijing, China during the
 637 2014 APEC campaign. The pie chart is the average composition of total detected organic compounds
 638 (TDOC) and the top number is the average mass concentration of TDOC of the whole study period.
 639



641

642 **Figure 4.** Compositions of total detected organic compounds (TDOC) in $\text{PM}_{2.5}$ during the 2014 APEC campaign.

643



645

646

Figure 5. Correlation analysis for oxalic acid (C_2) and sulfate in $\text{PM}_{2.5}$ during the whole 2014 APEC campaign. (a-c)

647

Concentrations of C_2 with sulfate, relative humidity (RH), and aerosol liquid water content (ALWC); (d, e)

648

sulfate and C_2 with aerosol acidity $[\text{H}^+]$ and (f) temperature with mass ratio of C_2 to total detected organic

649

compounds (C_2/TDOA).

650

651

652

653

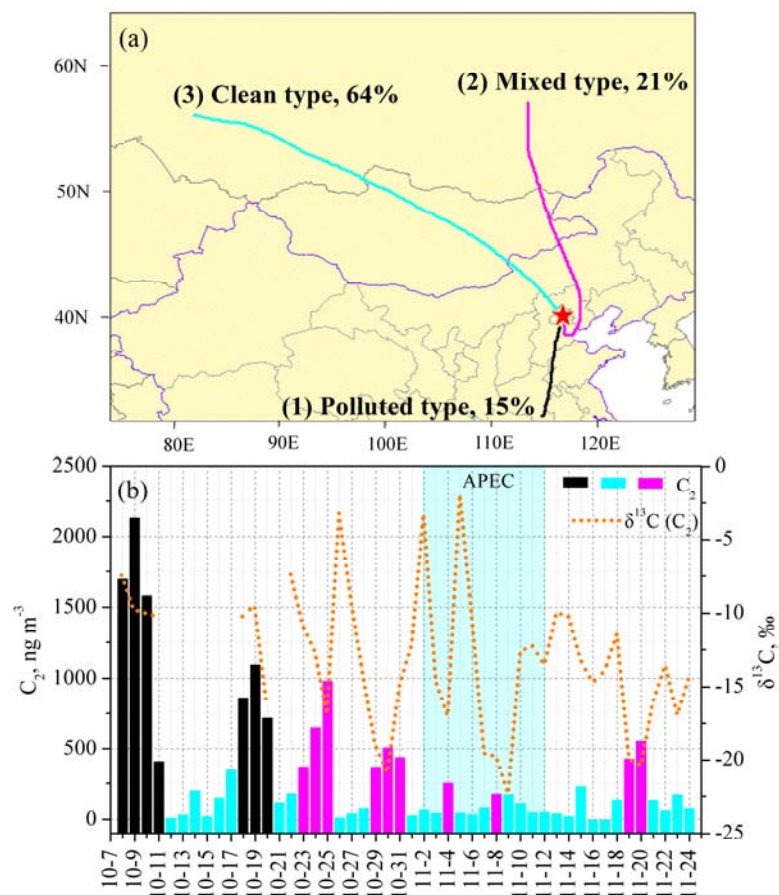
654

655

656

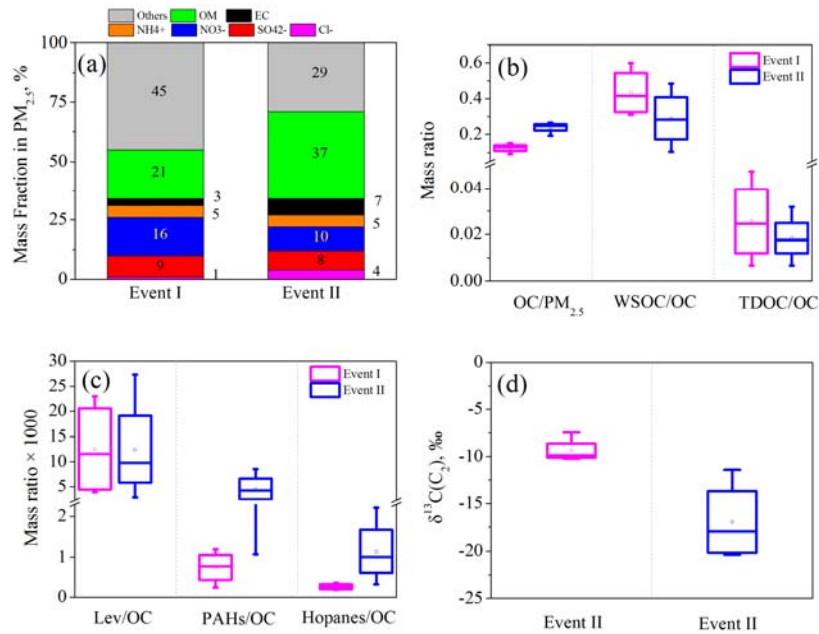
657

658



659
 660 **Figure 6.** (a) 72-h backward trajectories determined by the National Oceanic and Atmospheric Administration
 661 Hybrid Single Particle Lagrangian Integrated Trajectory (HYSPLIT) model arriving at the sampling site to
 662 reveal the major air mass flow types during the study period. Northwestern wind (light blue) was most
 663 frequently (64%), followed by northerly (21%, pink) and southerly (15%, black) and is defined as clean,
 664 mixed and polluted types, respectively (see the definitions in the text); (b) Time series of $\delta^{13}\text{C}$ values and
 665 concentration of oxalic acid during the whole study period (Colors in Fig. 6a are corresponding to those in
 666 Fig. 6b).

667
 668
 669
 670
 671
 672
 673



674
 675 **Figure 7.** Comparison of chemical composition of PM_{2.5} during two air pollution events. **(a)** Percentages of major
 676 species in PM_{2.5}; **(b, c)** mass ratios of major species and organic tracers in PM_{2.5}; **(d)** stable carbon
 677 isotope composition of oxalic acid (C₂) (Data about levoglucosan (Lev), PAHs and hopanes are cited
 678 from Wang et al (2016)).
 679